Spectrally compensated sum-frequency mixing scheme for generation of broadband radiation at 193 nm

Th. Hofmann, K. Mossavi, and F. K. Tittel

Department of Electrical and Computer Engineering, Rice Quantum Institute, Rice University, P.O. Box 1892, Houston, Texas 77251

G. Szabó

Department of Optics and Quantum Electronics, Attila József University, H-6720 Szeged, Dom ter 9, Hungary

A dispersively compensated scheme for sum-frequency mixing of broadband ultrashort laser pulses is reported. An increase of the bandwidth of the sum-frequency mixing process by 12 times compared with the noncompensated bandwidth of the given crystal has been demonstrated. Mixing radiation at 266 and 707 nm in a 1-mm-thick beta-barium metaborate crystal by using the compensated scheme results in an output bandwidth of 0.6 nm at 193 nm, which corresponds to a minimum output pulse duration of 90 fs.

The interest in various applications of far-UV and VUV laser pulses, such as ultrafast photodissociation studies of molecules or laser-induced fluorescence spectroscopy, has led to the development of methods to generate intense, coherent light in this part of the spectrum. A particularly important wavelength in this range is 193 nm, which is the wavelength of the ArF excimer laser. Ultrashort seed pulses at 193 nm can be amplified to gigawatt power levels.[1–3] Frequency tripling of the ArF laser has been reported to be a useful source of 64-nm radiation,[4] which can find important applications in biology and lithography. Short-pulse high-brightness ArF laser systems can be considered as a promising pump source for the production of x rays and laboratory-scale x-ray laser schemes,[5] but they may also play a fundamental role in extending the range of the ultrafast photodynamical studies of molecules[6–8] into the VUV region.

Different methods of generating 193-nm radiation have been reported: sum-frequency mixing (SFM) of UV and IR wavelengths in beta-barium metaborate[2,9] (BBO) and potassium pentaborate,[10] third-harmonic generation in Sr vapor,[1] and nonresonant[3] and near-resonant[11] difference-frequency mixing in Xe. Frequency mixing in gases generally requires extremely high pump intensities to achieve output energies sufficient for practical applications.[3]

For short pulses, the high dispersion of BBO makes it difficult to achieve high-efficiency SFM in the VUV range. By using the Sellmeier constants reported by Kato,[12] the spectral bandwidth for SFM at 193 nm using wavelengths of approximately 266 and 707 nm for a 1-mm-thick BBO crystal can be calculated to be approximately 0.05 nm, which corresponds to an approximately 1-ps minimum pulse duration, assuming a Gaussian pulse shape. Thus to generate 193-nm radiation with pulse durations in the subpicosecond range the crystal thickness should be well below

1 mm, which in turn results in decreased conversion efficiency.[2]

Several schemes for efficient frequency doubling[13–16] and tripling[17] of broadband ultrashort pulses by means of compensating the chromatic dispersion of the nonlinear crystal by angular spectral dispersion have been reported. The methods described in Refs. 13–16 were developed for frequency doubling; consequently, they cannot be used directly for SFM. The tripling scheme of Ref. 17 could also be used for SFM, but its single-beam input design would considerably increase the risk of damage to the dispersive element, and restriction of the input energy in order to avoid damage would limit the efficiency. In addition, as discussed below, the compensated mixing bandwidth is smaller when the input beams are collinear.

In this Letter we present a dispersive scheme especially designed for SFM that increases the spectral acceptance of a given crystal by more than a factor of 10. All the experimental details discussed below refer to a system that is designed to mix picosecond fourth-harmonic pulses from a Nd:YAG laser with femtosecond pulses from a dye laser (i.e., the UV input pulses are nearly monochromatic while the red input pulses are broadband); however, this arrangement can be adopted to other combinations of wavelengths and pulse durations by using the same design considerations. Furthermore, the scheme can be used not only with BBO in the VUV range, but also with other nonlinear crystals anywhere in the spectrum, including the far IR, where the spectral acceptance of the SFM process limits the conversion efficiency.

The experimental arrangement is depicted in Fig. 1. The 266-nm laser beam enters the BBO crystal directly, while the 707-nm beam is directed onto the reflection grating, where it is spectrally dispersed. The surface of the grating is imaged onto the crystal
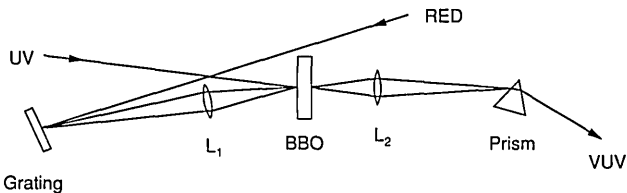
Fig. 1. Experimental arrangement for dispersively compensated SFM of broadband, ultrashort pulses.

by the lens (L₁) with a magnification that is chosen so that each of the spectral components of the red beam falls on the crystal at an angle that phase matches the 266-nm beam. The necessary magnification can be calculated by comparing the angular dispersion required by the crystal with that of the grating. By using the Sellmeier constants of Ref. 12 we obtain a crystal dispersion of 9.16 mrad/nm, whereas the dispersion of the 1200-line/mm grating used in the experiment is 1.672 mrad/nm, assuming an angle of incidence of 8.75°. (The incidence angle was chosen to achieve the highest efficiency with the given grating.) From these values we obtain 5.5 for the necessary magnification.

To achieve the largest output bandwidth, the central wavelength of the red beam was set slightly noncollinear with the 266-nm beam. The reason for this can be understood with the help of Fig. 2. (In the figure the indices of the k vectors are used in the following sense: the subscripts 1, 2, and 3 correspond to the central wavelength of 266, 707, and 193 nm, respectively, and the plus and minus, if present, indicate that the given vector belongs to a wavelength that is slightly longer or shorter than the central wavelength.) If the central component of the red and the UV beam were collinear, the length of the sum of the red and UV k vectors would be maximum practically at the central wavelengths [see Fig. 2(a)]. This would mean, however, that phase matching could only be achieved at wavelengths that are equal to or longer than the central VUV wavelength, because the length of the VUV k vector is a monotonic function of the frequency. This effect can be compensated for by aligning the central component of the red beam slightly noncollinear with the UV beam as indicated in Fig. 2(b).

As a result of the angular dispersion at the input of the crystal, the 193-nm sum-frequency output beam is also dispersed. It is recollimated by means of a lens (L₂) and a 60° fused-silica prism that is set to minimum deviation. Here the lens is again positioned so that the crystal plane is imaged onto the prism with the appropriate magnification to match dispersion. From the angular dispersion of 33.57 mrad/nm at 193 nm and a prism dispersion of 2.707 mrad/nm the required magnification is 12.4.

The imaging of the grating onto the crystal and the crystal onto the prism ensures (as can be seen by using Fermat's principle) that the optical path is equal for any of the red and VUV spectral components, provided that the lens aberrations can be neglected. This also means that the output pulse duration is expected to be the same as that of the red input pulse. This is, in fact, exactly what is needed

in the present experiments because the system is designed to mix picosecond fourth-harmonic pulses from a Nd:YAG laser with femtosecond red pulses from a dye-laser system. If, however, the UV input pulse duration were shorter, the scheme could be modified by dispersing the UV beam instead of the red beam.

In the arrangement depicted in Fig. 1 we used an $f = 100$ mm lens as L₁, an $f = 50$ mm fused-silica lens as L₂, and a 1-mm-thick BBO crystal cut to 76° phase matching, while the angle between the 266-nm beam and the central spectral component of the red beam was set at 7°.

The performance of the dispersively compensated SFM scheme was tested by simulating the broad bandwidth of the short input pulse with a tunable narrow-band laser. In this case the SFM energy is measured as a function of the VUV wavelength while the red laser is tuned, with the energy held constant. The advantage of this method is that the output bandwidth can be measured directly even if it is larger than that of the currently available shortest pulses at the given wavelength.

The measurements have been performed by using two nanosecond dye lasers pumped by the same XeCl excimer laser so as to avoid temporal jitter between the pulses. One of the dye lasers operated at a constant wavelength of 532 nm while the other was tuned around 707 nm. The dyes used in the red- and green-dye laser were Rhodamine 700 and Coumarin 540A (both dissolved in methanol), respectively. The output of the green-dye laser was frequency doubled by a 6.5-mm-thick BBO crystal that was cut for a 51° phase-matching angle and
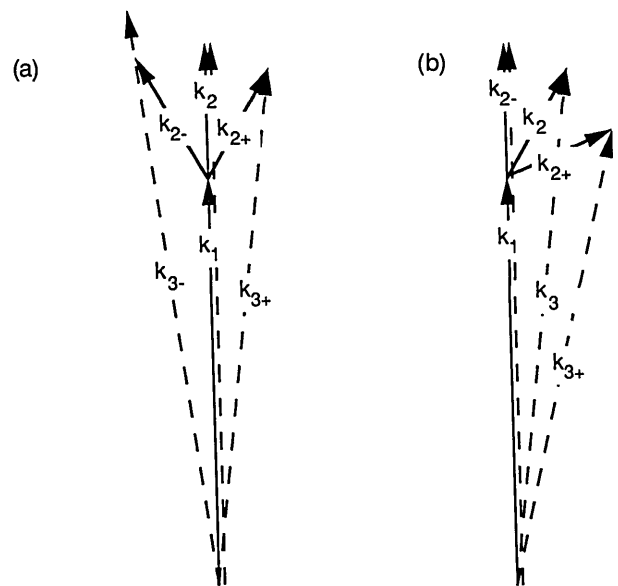

Fig. 2. Wave vectors showing the phase matching for dispersively compensated SFM scheme with central component of the 707-nm beam (a) collinear and (b) noncollinear with the 266-nm beam. The 1, 2, and 3 indices of the k vectors refer to the central wavelengths of 266, 707, and 193 nm, respectively. The plus and minus, if present, indicate that the given vector belongs to a wavelength that is slightly larger or smaller than the central wavelength.
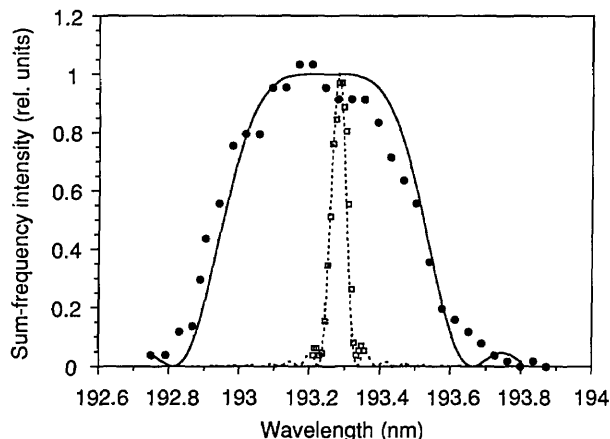
Fig. 3. Measured and calculated SFM spectral acceptance of a 1-mm-thick BBO crystal, uncompensated (squares and dashed curve) and compensated (circles and solid curve).

generated 200 μJ of energy at 266 nm. The output energy of the red-dye laser was 1 mJ.

For the intensity measurements at 193 nm, we used a solar-blind vacuum photodiode, whereas the wavelength was measured with a grating monochromator equipped with an optical multichannel analyzer.

The measured SFM bandwidths are shown in Fig. 3. The squares show the output of an uncompensated 1-mm-thick BBO crystal, and the circles represent the output of our dispersive scheme using the same crystal. Figure 3 also indicates the corresponding calculated SFM bandwidths by the dashed and solid curves, respectively. The calculations, showing good agreement with the measurements, have been performed in a low-conversion-efficiency limit simply by substituting the calculated phase mismatch Δk into

$$I_{\text{SFM}} \propto \frac{\sin^2 (\Delta k L/2)}{(\Delta k L/2)^2},\qquad(1)$$

where L is the crystal length.

From Fig. 3 it is evident that the dispersively compensated scheme increases the uncompensated SFM bandwidth of 0.05 to 0.6 nm (i.e., by a factor of 12), corresponding approximately to 90-fs minimum pulse duration. This also means that for a given output bandwidth (or pulse duration) the maximum allowable crystal length is 12 times longer than that without compensation. This increase in the useful crystal length is of fundamental importance because the SFM energy in the low-conversion-efficiency limit, which is generally valid for ultrashort pulses, is proportional to the square of the crystal length.

In preliminary experiments with 300-fs, 707-nm pulses we succeeded in generating 10 μJ of energy

at 193 nm with the broadest measured bandwidth of 0.22 nm, corresponding to 250-fs pulse duration. This energy is approximately two orders of magnitude higher than the seed pulse energy generated by SFM in Ref. 2, with comparable pulse duration.

In summary, we have developed a dispersively compensated scheme for SFM that increases the bandwidth of the SFM process by more than a factor of 10 compared with the noncompensated bandwidth of the given crystal. By using a 1-mm-thick BBO crystal we have measured an output bandwidth of 0.6 nm at 193 nm, corresponding to an output pulse duration of 90 fs.

References

1. H. Egger, T. S. Luk, K. Boyer, D. F. Muller, H. Pummer, T. Srinivasan, and C. K. Rhodes, Appl. Phys. Lett. **41**, 1032 (1982).
2. S. Szatmari and F. P. Schäfer, J. Opt. Soc. Am. B **6**, 1877 (1989).
3. J. H. Glownia, M. Kaschke, and P. P. Sorokin, Opt. Lett. **17**, 337 (1992).
4. H. Pummer, T. Srinivasan, H. Egger, K. Boyer, T. S. Luk, and C. K. Rhodes, Opt. Lett. **7**, 93 (1982).
5. M. Steyer, F. P. Schäfer, S. Szatmari, and G. Kühnle, Appl. Phys. B **50**, 265 (1990).
6. M. J. Rosker, M. Dantus, and A. H. Zewail, Science **241**, 1200 (1988).
7. J. H. Glownia, J. A. Misewich, and P. P. Sorokin, J. Chem. Phys. **92**, 3335 (1990).
8. T. R. Gosnell, A. J. Taylor, and J. L. Lyman, J. Chem. Phys. **94**, 5949 (1991).
9. W. Mückenheim, P. Lokai, B. Burghardt, and D. Basting, Appl. Phys. B **45**, 259 (1988).
10. R. E. Stickel and F. B. Dunning, Appl. Opt. **17**, 981 (1978).
11. A. Tünnermann, K. Mossavi, and B. Wellegehausen, Phys. Rev. A **46**, 2707 (1992).
12. K. Kato, IEEE J. Quantum Electron. **QE-22**, 1013 (1986).
13. G. Szabó and Zs. Bor, Appl. Phys. B **50**, 51 (1990).
14. O. E. Martinez, IEEE J. Quantum Electron. **25**, 2464 (1989).
15. T. R. Zhang, H. R. Choo, and M. C. Downer, Appl. Opt. **29**, 3927 (1990).
16. R. A. Cheville, M. T. Reiten, and N. J. Halas, Opt. Lett. **17**, 1343 (1992).
17. M. D. Skeldon, R. S. Craxton, T. J. Kessler, W. Seka, R. W. Short, S. Skrupsky, and J. M. Soures, IEEE J. Quantum Electron. **28**, 1389 (1992).